ACS APPLIED NANO MATERIALS

www.acsanm.org Article

Functionalized Single-Walled Carbon Nanotubes and Nanographene Oxide to Overcome Antibiotic Resistance in Tetracycline-Resistant *Escherichia coli*

Jordan A. Carver,[#] Audrey L. Simpson,[#] Ria P. Rathi,[#] Nerica Normil,[#] Amy G. Lee,[#] Madison D. Force,[#] Katherine A. Fiocca,[#] Christopher E. Maley,[#] Kara M. DiJoseph,[#] Abigail L. Goldstein,[#] Amin A. Attari,[#] Haley L. O'Malley, Jaclyn G. Zaccaro, Noël M. McCampbell, Christina A. Wentz, Jessica E. Long, Lilly M. McQueen, Francis J. Sirch, Broderick K. Johnson, Molly E. Divis, Matthew L. Chorney, Steven L. DiStefano, Holly M. Yost, Brandon L. Greyson, Emily A. Cid, Kyumin Lee, Codi J. Yhap, Michelle Dong, Dayna L. Thomas, Brittany E. Banks, Regan B. Newman, Jailene Rodriguez, Alix T. Segil, Justin A. Siberski, Anthony L. Lobo, and Mark D. Ellison*

Cite This: https://dx.doi.org/10.1021/acsanm.0c00677 Read Online

ACCESS | Metrics & More | Article Recommendations | Supporting Information

ABSTRACT: Antibiotic resistance is a significant and growing public health problem. This work investigated the use of two different carbon nanomaterials, single-walled carbon nanotubes (SWNTs) and nanographene oxide (NGO), as a means of delivering the antibiotic tetracycline to a strain of *Escherichia coli* bacterium with an efflux pump resistance mechanism. Both SWNTs and NGO carrying tetracycline were found to inhibit the resistant strain of *Escherichia coli*, though the amount of tetracycline delivered was much lower than the minimum inhibitory concentration of free tetracycline. Attachment of the tetracycline to the nanomaterials was found to be necessary for the inhibition of bacterial growth, indicating that the nanomaterials were transporting the antibiotic into the cells and subverting the efflux pump. SWNTs were observed to have greater efficacy in delivering tetracycline than graphene oxide, which is attributed to the SWNTs' needle-like shape. This work demonstrates both the use of carbon nanomaterials as antibiotic-delivery vehicles and the effect of nanomaterial shape on their efficacy. More importantly, it demonstrates that nanomaterials can successfully extend the life of existing antibiotics, making them an important tool for combatting antibiotic resistance mediated by an efflux pump mechanism.

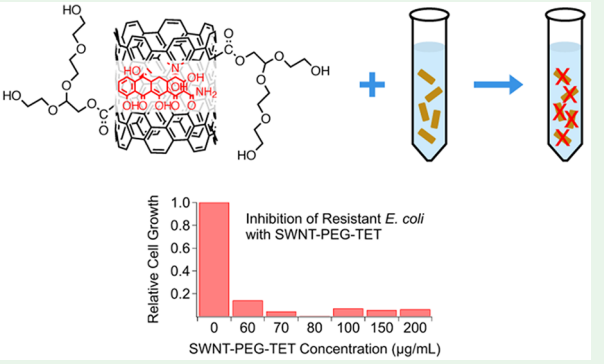

KEYWORDS: *carbon nanotubes, graphene, tetracycline, Escherichia coli, antibiotic resistance*

Downloaded via TEMPLE UNIV on April 13, 2020 at 14:21:47 (UTC).
See https://pubs.acs.org/sharingguidelines for options on how to legitimately share published articles.

INTRODUCTION

Antibiotic resistance is one of the most significant health concerns facing humanity. Each year in the United States, approximately 2 million people contract an antibiotic-resistant infection, and roughly 23 000 people die from such infections.[1] Furthermore, the economic impact of antibiotic-resistant infections is estimated to be $20−$35 billion each year.[1] On an international scale, more than 700 000 people die each year from antibiotic-resistant infections.[2] Additionally, the World Bank estimates that the death toll could reach 10 million annually by 2050 if no progress is made.[3] Indeed, the World Health Organization lists antibiotic resistance as one of the greatest threats to "health, food security, and development".[2] As microbes develop resistance to current antibiotics, the high cost of research and development makes the discovery and development of new antibiotics a stiff economic challenge for pharmaceutical companies.[4] The time from the start of research through regulatory approval and clinical trials is estimated to be two decades,[5] making the development of new antibiotics all the more challenging. Because of the wide-scale nature of the problem, a widespread effort must be exerted to combat antibiotic resistance.

In a recent survey of 67 countries across 5 continents, *E. coli* was one of the five most-reported resistant bacteria.[6] This Gram-negative pathogen is responsible for many foodborne

Received: March 10, 2020
Accepted: April 2, 2020
Published: April 2, 2020

© XXXX American Chemical Society

illnesses and other infections. In this work, tetracycline-resistant *E. coli* were produced by using the pBR322 plasmid to transform the DH5α strain of *E. coli*. This plasmid was assembled from three different naturally occurring plasmids and contains both a tetracycline-resistance gene, *tetA*, and an ampicillin-resistance gene.[7] The *tetA* gene codes for an efflux pump, a transmembrane protein that expels tetracycline[8] by exchanging a monocationic metal−tetracycline complex inside the cell with a proton outside the cell.[9] This system removes tetracycline before it can interact with its target, the ribosome, sparing the organism from the effect of the antibiotic.

Nanomaterials are an area of opportunity in the battle against antibiotic resistance, and research has already revealed the antimicrobial properties of some nanomaterials. For instance, Ag and Au nanoparticles as well as nanoparticles made of other metals, semiconductors, and metal oxides, have been shown to effectively kill or damage many different species of bacteria.[10−12] There has also been much work on using a variety of nanomaterials for the delivery of therapeutic agents,[13−32] including anticancer[13−18] and antifungal drugs.[31,32]

Carbon nanomaterials, particularly carbon nanotubes and graphene, have been well-researched and found to be effective for drug delivery, as summarized in several review articles.[19,20,23,27,29,30] However, only a few studies have been published about the use of carbon nanomaterials to deliver antibiotics. In one study, Assali et al. covalently attached ciprofloxacin to SWNTs and exposed *Staphylococcus aureus, Pseudomonas aeruginosa*, and *E. coli* to those functionalized SWNTs.[33] They found that their Cipro-SWNTs were 16 times more effective than free ciprofloxacin toward *S. aureus* and *P. aeruginosa* and 8 times more effective toward *E. coli.*

Thakur et al. reported the use of fluorescent carbon dots for delivery of ciprofloxacin (Cipro@C-dots) to *E. coli, Bacillus subtilis, S. aureus,* and *P. aeruginosa.*[34] They found that their Cipro@C-dots were effective against ciprofloxacin-sensitive strains of the Gram-positive and Gram-negative bacteria they tested. They also found evidence that the C-dots exhibited some antibacterial activity and suggested that synergy between the nanomaterial and antibiotic could explain the observed effectiveness.

In 2010, Ghosh et al. used para-aminobenzoic acid-functionalized graphene oxide (GO) to deliver tetracycline to resistant *E. coli.*[35] However, they did not report testing the separate addition of graphene oxide and tetracycline, so their studies could not rule out that graphene oxide damage to the cell membranes allowed tetracycline to enter the cells. Additionally, Gao et al. investigated the effect of GO on the sensitivity of *E. coli,* and *S. aureus* to three different antibiotics: lincomycin hydrochloride, chloramphenicol, and gentamycin sulfate.[36] They found that exposing the bacteria to GO before being treated with the antibiotics generally increased the effectiveness of lincomycin and chloramphenicol toward the bacteria. They attributed this result to GO-induced damage to the cell membranes. These findings by Gao et al. suggest that Thakur et al.'s results with Cipro@C-dots and Ghosh et al.'s results with graphene oxide could indeed arise from damage that the nanomaterials inflict on bacterial cell membranes. This is also in agreement with findings that graphene oxide has antibacterial properties.[37,38]

Very recently, Khazi-Syed et al. used SWNTs to deliver doxycycline and methicillin to methicillin-resistant *Staphylococcus epidermidis.*[39] They found that the SWNT/methicillin nanocomposite was 40 times more effective at inhibiting the bacteria than methicillin alone, whereas the SWNT/doxycycline complex was only slightly more effective than just the antibiotic. They also showed that their SWNT/antibiotic complexes were less toxic to mammalian cells than antibiotics alone.

These results clearly illustrate the potential for carbon nanomaterials to deliver antibiotics and the importance of understanding the toxicity of nanomaterials toward cells. In general, previous research has determined that several factors play a key role in determining the level of toxicity of SWNTs and graphene: (1) the size and shape of the nanomaterial, (2) the degree of functionalization of the nanomaterial, (3) the type of cell involved, and (4) the degree of agglomeration of the nanomaterial.[40,41] Specifically, nonfunctionalized SWNTs exhibit detrimental effects on both human[40,42−45] and bacterial[46,47] cells, as well as bacteria biofilms.[48] Likewise, graphene and graphene oxide can cause cellular damage and disruption in mammalian[49−52] and bacterial cells.[37,53] Conversely, functionalized SWNTs[41,54,55] and graphene[49−51,56] are much less toxic to a variety of cell types. These results demonstrate the importance of the type and degree of functionalization and the cell type on the toxicity of carbon nanomaterials. Although previous work can provide some guidance, the cytotoxicity of each nanomaterial is best determined on a case-by-case basis.

Given the effectiveness of carbon nanomaterials in delivering drugs, we chose to investigate the use of SWNTs and NGO to deliver tetracycline to antibiotic-resistant *E. coli.* Tetracycline is a common, broad-spectrum, bacteriostatic antibiotic that is effective against Gram-negative bacterial infections, which are more resistant to treatment.[1,5] Moreover, tetracycline and its derivatives are being employed more frequently as additional Gram-negative bacteria exhibit resistance to other antibiotics, and the tetracycline family is the third-most-widely prescribed class of antibiotics in the world.[1] Tetracycline binds to the 30s subunit of the ribosome and inhibits protein synthesis.[57,58] Specifically, X-ray diffraction shows that tetracycline binds in a space 20 Å wide and 7 Å deep, so the antibiotic must be able to detach from the delivery system to successfully bind to the ribosome. Therefore, our goal was to construct a nanomaterial−antibiotic system that would release the antibiotic within the cell. Numerous studies have shown that tetracycline has an affinity for carbon nanotubes[59] and graphene.[60] Both of these nanomaterials will adsorb tetracycline from aqueous solutions, indicating that noncovalent attachment is possible under such conditions. We hypothesized that noncovalent attachment would be strong enough to deliver tetracycline into the cells but not so strong that the tetracycline could not be released within the cells. Our results demonstrate the effectiveness of functionalized SWNTs and NGO to deliver tetracycline to the antibiotic-resistant *E. coli*.

EXPERIMENTAL SECTION

SWNTs Preparation. SWNTs were purchased from Carbon Solutions, Inc. (P2-SWNT, > 90% carbonaceous purity). These SWNTs are typically between 2 and 5 μm long. Shorter SWNTs are easily dispersed in aqueous solutions and better suited to enter cells.[43,61] Therefore, a strong acid treatment was used to cut the SWNTs into segments of 500 nm or shorter.[62] First, a 3:1 mixture by volume of concentrated sulfuric and nitric acids was prepared. SWNTs were added in a proportion of 1 mg of SWNTs to 10 mL of acid mixture. Next, the reaction flask was submerged in ice water in an ultrasonic bath, (Elma S30H Elmasonic) that was located in a cold

https://dx.doi.org/10.1021/acsanm.0c00677
ACS Appl. Nano Mater. XXXX, XXX, XXX−XXX

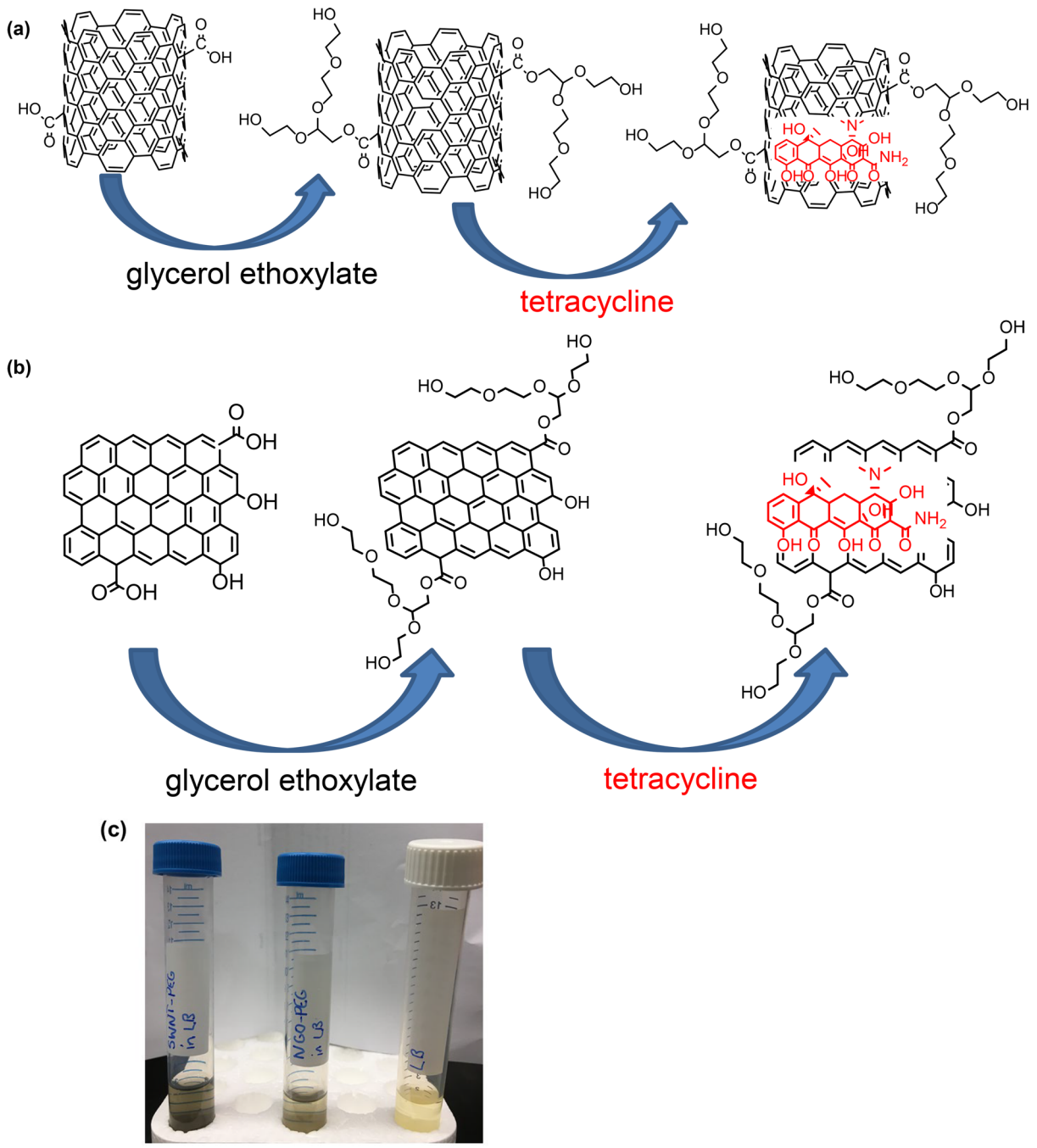

Figure 1. (a) Schematic of PEGylation of SWNTs followed by TET attachment. (b) Schematic of PEGylation of NGO followed by TET attachment. (c) SWNT−PEG (left), NGO−PEG (middle) dispersed in LB broth, both at concentrations of 100 μg/mL. Pure LB shown on right for comparison.

room maintained at 4 °C. The ice in the bath was replenished every 30−45 min to keep the temperature below 8 °C. Close temperature control was necessary because Shuba et al. reported that if the temperature exceeded 8 °C, significant degradation of the SWNTs would occur.[62] Next, the SWNTs were sonicated for 12 h. After sonication, the reaction flask was removed from the ultrasonic bath, and the acid was neutralized using a solution of saturated sodium carbonate. After neutralization, the suspension of cut SWNTs was filtered using a 0.2-μm filter membrane (Millipore), and then the filtrate was washed with copious amounts of deionized (DI) H_2O to remove the Na_2SO_4 and $NaNO_3$ byproducts from the neutralization. After being washed, the cut SWNTs were placed in a covered Petri dish and allowed to dry in ambient conditions.

The cut SWNTs were characterized using transmission electron microscopy (TEM; LVEM 25, 25 kV accelerating voltage). Multiple images of each nanomaterial were acquired to obtain reliable statistics on the size measurements. Images were calibrated with a scale bar and analyzed using ImageJ.[63] The sizes of at least 100 distinct particles (SWNTs or NGO) were measured, and the averages and standard deviations of the size measurements were calculated. This analysis (see Supporting Information Figures S1 and S2) shows that the raw SWNTs had a length of 4.0 ± 1.7 μm. The cut SWNTs had a length of 1.1 ± 0.4 μm. The cut SWNTs had a much shorter average length and a much narrower distribution of lengths than the untreated SWNTs. However, the average length of the SWNTs after acid treatment was somewhat greater than that found by Shuba et al., which is attributed to the shorter reaction time used in this work.

https://dx.doi.org/10.1021/acsanm.0c00677
ACS Appl. Nano Mater. XXXX, XXX, XXX−XXX

Bacterial Culture Preparation. Broth cultures were prepared for both the *E. coli* DH5α and DH5α-pBR322 strains. Three milliliters of LB broth was inoculated with bacteria of each strain. The cultures were incubated overnight at 37 °C at 150 rpm agitation. Each strain grew to an absorbance of approximately 1.0 at 600 nm.

Synthesis of SWNT−PEG and NGO−PEG. Covalent attachment of poly(ethylene glycol), (PEG) also known as PEGylation,[18] is a very useful method for increasing the solubility and biocompatibility of nanomaterials.[56] Therefore, to increase the water solubility of the SWNTs and NGO, PEG was covalently attached to the SWNTs and NGO in solution using an esterification reaction similar to that reported by Liu et al.[18] in which carboxylic acid groups on the cut SWNTs or NGO react with hydroxyl groups on the PEG to form an ester that covalently attaches the PEG to the SWNTs (Figure 1a). Specifically, the cut SWNTs or the NGO (Carbon Solutions, Inc., product code GO) were added to DI H_2O in a ratio of 1 mg of SWNTs to 1 mL of DI H_2O. To this solution was added 8.5 μg of glycerol ethoxolate (Sigma-Aldrich, average $M_n \approx 1000$) for every 1 mL of DI H_2O. The mixture was bath sonicated for 5 min to thoroughly disperse the SWNTs or NGO. Next, *N*-(3-(dimethylamino)propyl)-*N*′-ethylcarbodiimide hydrochloride (EDC, Sigma-Aldrich, 98%) was added in the same mass as the nanomaterial, and the mixture was sonicated for 30 min. Finally, three times the mass of EDC as previously added was added to the mixture. This mixture was then stirred for 24 h in a cold room maintained at 4 °C. At this stage, the preparation of the SWNTs and NGO differed. The preparation of the SWNTs is described here, and the preparation of the NGO is described in the next paragraph. After being stirred for 24 h, the mixture was filtered using the 0.2-μm membrane. The attachment of PEG was verified using ^{1}H nuclear magnetic resonance (NMR; Bruker Avance 300 MHz) spectrometry with all samples dissolved in CD_3COCS_3, as well as Fourier transform infrared (FTIR; Nicolet 6700) spectroscopy (see Figures S6 and S7 and Table S2). The PEG-attached SWNTs or NGO (SWNT−PEG, NGO−PEG) were collected in a sterile covered plate and stored at room temperature. The SWNT−PEG was also analyzed by TEM. The lengths of the PEGylated SWNTs were found to be 1.1 ± 0.6 μm, which is essentially identical to those of the cut SWNTs.

Continuing with the description of the NGO preparation, after 24 h on the stir plate, phosphate buffered saline (PBS) at an amount equal to 1/20 of the original solution volume and deionized water (1/6 of the original solution volume) were added to the flask and swirled. The resulting solution was centrifuged at 9000 rpm for 1 h. After centrifugation, the NGO−PEG was collected by filtration through a 0.2-μm membrane (Millipore). The attachment of PEG to the NGO was confirmed by NMR and FTIR spectroscopies. TEM images of the NGO and NGO−PEG were also collected and analyzed (see Figures S1 and S3). For size analysis, these forms of graphene were approximated as being rectangular in shape, which is close to the observed shape of an overwhelming majority of particles observed. For NGO, the average dimensions were found to be 86 ± 51 nm × 25 ± 13 nm, and for NGO−PEG, the average dimensions were 69 ± 32 nm × 33 ± 16 nm. Both SWNT−PEG and NGO−PEG dispersed well in LB broth at concentrations of 100 μg/mL, as shown in Figure 1c.

Functionalization of SWNT−PEG and NGO−PEG with TET. Tetracycline (TET) is light-sensitive, so every effort was made to minimize its exposure to light during all experiments. As a general practice, the room lights were turned off, and all containers containing TET were wrapped in aluminum foil. First, the SWNT−PEG or NGO−PEG was sterilized in an autoclave, and all subsequent procedures were carried out under sterile conditions. For the noncovalent attachment of TET, different mass ratios of TET to SWNT−PEG and NGO−PEG were tested. It was found that a mass ratio of 1.0−1.5 resulted in the maximum amounts of attached TET. Typically, 0.014 g of tetracycline (Sigma-Aldrich, >98.0%) and an equal amount of SWNT−PEG or NGO−PEG were measured and added to DI H_2O in a ratio of 1 mg of SWNT−PEG to 1 mL of DI H_2O. The tetracycline was dissolved in minimal amounts of 70% ethanol (1−1.5 mL). The tetracycline solution was added to the SWNT−PEG solution in an aluminum-foil-covered flask and stirred for 18 h in a 4 °C cold room. After a period of 18 h, the solution was filtered using the same filter apparatus as previously mentioned, and the tetracycline-attached SWNT−PEG (SWNT−PEG−TET) or NGO−PEG (NGO−PEG−TET) was collected and stored in an aluminum-foil-wrapped covered plate in a −20 °C freezer. The filtrate was saved and stored in a foil-wrapped 50 mL conical tube in a refrigerator for later analysis of the amount of TET attached to the SWNT−PEG or NGO−PEG. The attachment of TET was verified by NMR and FTIR spectroscopies (see Figures S6 and S7).

Quantification of Amount of TET Attached to SWNT−PEG or NGO−PEG. The filtrate saved from the previous procedure was diluted by a factor of 100 (20 μL of filtrate diluted to 2 mL with DI H_2O) to bring the absorbance within the linear response range. A blank was made with DI H_2O and 70% ethanol, matching the filtrate solvent. A set of standard solutions was also developed at concentrations from 0.002 μg/mL to 0.010 μg/mL to create a standard absorbance plot. Using a UV−vis spectrophotometer (Jasco V-670), the absorbance peak of TET at 380 nm in each solution was measured, and a standard curve was constructed using the standard solutions noted above. The absorbance peak for the diluted filtrate solution was then measured and plotted against the standard curve, permitting the calculation of the amount of TET remaining in the filtrate. Then, by subtraction, the amount of TET attached to the nanotubes was calculated. For five trials, the average mass percentage of TET in the SWNT−PEG−TET was 55%.

The same process was performed for NGO−PEG−TET. For five trials, the NGO−PEG−TET was found to average 50% TET by mass, which is consistent with the results of Zhang et al.[64]

Incubations of SWNT−PEG−TET with *E. coli*. To test the efficacy of the SWNT−PEG−TET and NGO−PEG−TET solutions compared with the free TET, SWNT−PEG−TET or NGO−PEG−TET solutions were prepared to find the new minimum inhibitory concentration range. For the DH5α strain, LB broth cultures with tetracycline concentrations of 0, 5, 10, and 15 μg/mL were prepared. For the DH5α-pBR322 strain, broth cultures with tetracycline concentrations of 0, 50, 60, 70, 80, 100, 150, 200, and 250 μg/mL were produced. Cultures were inoculated with 0.1 mL of overnight culture of each strain, and then covered in aluminum foil in 50 mL conical tubes and incubated overnight at 37 °C while being agitated at 150 rpm. The same process was followed using the NGO−PEG−TET.

Quantifying the Inhibition of *E. coli* by SWNT−PEG−TET and NGO−PEG−TET. After each solution had been incubated for 20 h, its absorbance was read using a spectrophotometer (Thermo Scientific Genesys 20) set at 600 nm. The absorbance values gave a relative value of bacterial growth, so comparisons to control solutions indicated how strongly bacteria growth was inhibited. However, the SWNT−PEG in the solutions may also absorb light, making absorbance values less accurate. Therefore, to further quantify inhibition, viable plate counts were performed on solutions at each concentration. After overnight growth, cultures were diluted by powers of ten from 10^{-1} to 10^{-8}, and 100 μL of each concentration was pipetted onto separate plates, which were then placed into the incubator at 37 °C for 24 h. After 24 h, the plates were removed from the incubator and photographed, and the numbers of colonies that grew were counted. In accordance with convention, plates with more than 200 colonies were designated too numerous to count (TNTC). For NGO−PEG−TET, absorbance measurements and viable counts were performed in the same manner as was described above for SWNT−PEG−TET.

Test of Separate Addition of SWNT−PEG and NGO−PEG and TET. To determine whether TET attachment to SWNT−PEG or NGO−PEG is necessary for the inhibition of resistant bacteria, SWNT−PEG and TET were added independently to the bacterial solutions, and the growth of bacteria after 24 h was measured. One stock solution of 1.0 mg/mL SWNT−PEG and one stock solution of 1.0 mg/mL TET were made.

Two sets of incubations were made; the first set contained SWNT−PEG and TET, whereas the second set only contained

https://dx.doi.org/10.1021/acsanm.0c00677
ACS Appl. Nano Mater. XXXX, XXX, XXX−XXX

SWNT−PEG. Both sets were tested with *E. coli* DH5α and DH5α-pBR322. Overnight cultures of the *E. coli* strains were prepared as described above. SWNT−PEG stock solution was pipetted into LB broth in sterile 50 mL conical tubes and 0.1 mL of the overnight cultures to result in 100 μg/mL concentrations of SWNT−PEG. After 1 h of incubation, TET was added to each conical tube to make its concentration 100 μg/mL. This would allow the SWNT−PEG to interact with the bacteria separately prior to the addition of TET. The second set was prepared by adding only specific volumes of SWNT−PEG. Both sets were incubated overnight as described previously.

After overnight incubation, the absorbance of each solution was measured using a spectrophotometer set at 600 nm. Because the measured absorbances indicated no inhibition of resistant bacteria with SWNT−PEG alone or with separately added TET, further viable counts were not performed. This procedure was repeated for NGO−PEG.

Lactate Dehydrogenase Assay of Nanomaterial Cytotoxicity. A lactate dehydrogenase (LDH) assay kit (Invitrogen) was used to assess the cytotoxicity of SWNT−PEG and NGO−PEG toward *E. coli.* The process exposes *E. coli* to the substance being tested and includes a control exposure to water and an LDH control. LDH catalyzes the reaction that produces pyruvate from lactate through the reduction of NAD+ to NADH. Then, NADH reduces a tetrazolium salt to formazan, which is red and can be quantified by absorbance measurements. Cell exposures were performed in triplicate in a 96-well plate, and absorbances at 450 nm were measured on a plate reader (Molecular Devices SpectraMax F5).

Live/Dead Cell Quantification. A bacterial viability assay kit (Abcam ab189818) containing two fluorescent dyes was used to quantify the percentages of living and dead cells after exposure to the nanomaterials. One dye enters all cells, allowing the total number of cells to be determined. The other dye enters only dead cells, allowing the number of dead cells to be directly quantified. From these values, the percentage of dead cells can be calculated, and from that number, the percentage of live cells is readily determined. Bacteria cells were grown from cultures according to the steps described above. They were then exposed to SWNT−PEG or NGO−PEG at concentrations of 100 μg/mL for 1 h and 24 h. A control group was not exposed to any nanomaterials. After the given exposure time, the cells were centrifuged at 10000*g* for 10 min, resuspended in wash buffer, and then incubated at room temperature, centrifuged, washed, and resuspended for several stages according to the assay kit protocol. A control dead cell sample was prepared by suspending 1 mL of cell solution in 5 mL of 70% isopropyl alcohol. Finally, 1.0-μL aliquots of total cell dye stain and dead cell dye stain were then added to each sample tube. The total number of cells was measured by fluorescence at 525 nm (490 nm excitation), and the number of dead cells was measured by fluorescence at 617 nm (535 nm excitation). (Molecular Devices FilterMax F5)

Hemolysis Test of Nanomaterial Biocompatibility. Red blood cells (RBC) from sheep blood (Hardy Diagnostics, Santa Maria, CA) were used to assess biocompatibility and potential toxicity of the nanomaterials. These red blood cells are used widely as a proxy for human RBC in measuring the hemolytic activity of toxins produced by bacteria pathogenic to humans,[65,66] membrane-active peptides,[67,68] noninfectious hemolytic diseases,[69,70] and membrane-disrupting compounds such as bile salts and aliphatic alcohols.[71,72] Directly relevant to this study, sheep RBCs have been used to measure the extent of membrane disruption by polymeric nanoparticles designed to deliver antitumor drugs.[73] In studies in which human and sheep RBCs were compared directly[66,67,72] the sheep RBCs were more susceptible to lysis, suggesting that human cells might be more resistant than sheep RBCs to membrane damage; thus, the extent to which we saw damage to sheep RBCs due to SWNT−PEG and NGO−PEG would likely occur to a lesser degree to human cells. Cells were centrifuged to form a pellet, washed three times with a sterile 1.0% saline solution, and then resuspended in 1.0 mL of that same saline solution. SWNT−PEG and NGO−PEG were added to solutions of the suspended red blood cells to yield a final nanomaterial concentration of 100 μg/mL and 0.90% saline concentrations. Control solutions of red blood cells in 0.90% saline solution were also made. Full lysis was achieved by suspending the red blood cells in 1.0 mL of distilled water. Absorbances were measured at 575 nm to quantify the amount of hemoglobin released. (Molecular Devices FilterMax F5)

RESULTS AND DISCUSSION

Biocompatibility and Cytotoxicity Results. Control experiments showed that neither SWNT−poly(ethylene glycol) (PEG) nor NGO−PEG, at the maximum concentrations used in the research, inhibit bacterial growth of both the nonresistant and the resistant strains of *E. coli* (see Figure S4). Because dead or damaged bacteria absorb light just as readily as healthy bacteria, absorbance measurements were corroborated with viable count experiments and live/dead cell assays. In viable count experiments, bacteria exposed to SWNT−PEG or NGO−PEG at a concentration of 100 μg/mL were compared to a control incubated without any nanomaterial (see Table S1). Very little difference was observed between the bacteria not exposed to nanomaterials and those exposed to the nanomaterials. Specifically, the control DH5α-pBR322 had $(1.1 \pm 0.1) \times 10^9$ colony forming units per milliliter (cfu/mL). Similarly, the DH5α-pBR322 exposed to NGO−PEG had $(1.1 \pm 0.1) \times 10^9$ cfu/mL, while the DH5α-pBR322 exposed to SWNT−PEG had $(8.9 \pm 0.1) \times 10^8$ cfu/mL. Using Student's *t*-test, the NGO−PEG cfu/mL are not statistically significantly different from the control, whereas those for the SWNT−PEG were statistically significantly different from the control. The bacteria exposed to SWNT−PEG had slightly fewer cfu/mL, which could indicate a small amount of toxicity toward the bacteria, possibly due to incomplete PEGylation of the nanotubes. However, the effect is small, and these results indicate that exposure to the nanomaterials does not cause a large decrease in viability of the bacteria cells.

Additionally, the results of live/dead cell assay experiments are shown in Table 1. The average percentages and standard deviations of three measurements are reported. After 1 h the percentages of *E. coli* exposed to SWNT−PEG and NGO−PEG that are dead are not significantly different than those of the control *E. coli.* However, the bacteria exposed to SWNTs do exhibit a greater percentage of dead cells, indicating that the PEGylation decreases the nanomaterials' toxicity. After 24 h, the percentages of the dead bacteria exposed to any of the nanomaterials are not significantly different than the control group of bacteria, indicating that the nanomaterials are not causing significant amounts of cell death.

Table 1. Percent of DH5α-PBR322 *E. coli* cells that were dead after 1-h and 24-h exposures to 100 μg/mL of SWNTs, SWNT−PEG, and NGO-PEG

material	1 h	24 h
control	4.0 ± 1.0%	11 ± 1%
SWNTs	10 ± 2%	11 ± 1%
SWNT−PEG	5.3 ± 2.0%	10 ± 1%
NGO−PEG	8.6 ± 3.2%	10 ± 1%

Hemolysis experiments found very little lysis of sheep RBC by any of the nanomaterials, as shown in Table 2. Our hemolysis results are in good agreement with those of Canape et al.,[74] who tested oxidized SWNTs and PEG-functionalized SWNTs on rat and human RBC. Additionally, Heo et al. found

https://dx.doi.org/10.1021/acsanm.0c00677
ACS Appl. Nano Mater. XXXX, XXX, XXX−XXX

Table 2. Percent of Red Blood Cells That Were Hemolyzed after 1-h and 24-h Exposures to 100 μg/mL of SWNTs, SWNT−PEG, and NGO-PEG

material	1 h	24 h
control	0.35 ± 0.05%	0.64 ± 0.04%
SWNTs	1.5 ± 0.5%	2.7 ± 0.4%
SWNT−PEG	3.1 ± 0.6%	2.5 ± 0.5%
NGO−PEG	3.6 ± 1.0%	2.4 ± 0.4%

that individually dispersed SWNTs exhibited <10% hemolysis. Similarly, Sasidharan et al. found that unfunctionalized NGO showed <1% hemolysis.[75] Because <10% lysis has been reported as being nonhemolytic,[76] our results indicate very good biocompatibility of both the SWNT−PEG and NGO−PEG. It is also worth noting that several studies have found that sheep RBC are more easily lysed by hemolytic toxins than human RBC.[67,72] Therefore, human RBC would likely undergo even less hemolysis than was found in our experiments.

Finally, lactate dehydrogenase (LDH) activity experiments showed that the LDH activities of solutions with bacteria exposed to 100 μg/mL concentrations of either nanomaterial are not greater than or even qualitatively different from those of bacteria exposed to water (see Figure S5). These results indicate that the nanomaterials do not cause a significant release of LDH from the bacteria, suggesting that the PEGylated nanomaterials do not significantly damage the bacteria. Taken all together, these control experiments demonstrate that neither SWNT−PEG nor NGO−PEG does significant damage to or significantly inhibits the growth of the *E. coli*. We do note that previous research found that non-PEGylated SWNTs are toxic to *E. coli*[47,77] and *Salmonella typhimurium*.[78] Additionally, unfunctionalized NGO is toxic toward bacterial cells.[37,38] However, our control experiments do not show any evidence that PEGylated SWNTs or NGO kill or inhibit the bacteria. We attribute the difference between the results in the literature and the ones presented here to the PEGylation performed on the nanomaterials in this work.

Results of Nanomaterial Action Against *E. coli*. NMR and IR spectra confirmed the attachment of PEG and tetracycline (TET) to SWNTs and NGO, with the NMR peaks closely matching the literature values[79,80] (see Figure S6). Using UV−vis quantification of TET in the filtrate, the SWNT−PEG−TET was observed to be about 55% TET by mass, and the NGO−PEG−TET was observed to be about 50% TET by mass. Tetracycline is slightly soluble in water when not in its hydrochloride form. Here we used TET alone, allowing the TET to remain attached to the SWNTs or NGO in the LB broth. The NGO−PEG−TET and the SWNT−PEG−TET were found to inhibit the growth of both the nonresistant and the resistant strains of *E. coli*. Figure 2a−c shows the relative growth, normalized to the growth with no nanomaterial present, of the resistant strain for free TET and the nanomaterials attached to TET. The minimum inhibitory concentrations (MIC) of free TET for DH5α and DH5α-pBR322 were determined to be 10 and 200 μg/mL, respectively. Conversely, for DH5α-pBR322 the MICs of SWNT−PEG−TET and NGO−PEG−TET were found to be 70 and 150 μg/mL, respectively. Using the mass percentages of TET in the nanomaterials, the amounts of TET per milliliter of solution were 38 and 75 μg/mL, respectively. It is clear from these experiments that the nanomaterials bound to TET are much more effective against the resistant *E. coli* than free TET alone. These MIC data demonstrate that the nanomaterials enhance the effectiveness of TET toward the resistant bacteria.

This conclusion is supported by the viable count experiments, the results of which are shown in Figure 3a−d and Tables 3 and 4. For the SWNT−PEG−TET, inhibition occurs at concentrations greater than 70 μg/mL (effective TET concentration of about 38 μg/mL). Likewise, for the NGO, the bacteria are not strongly inhibited at a total concentration of

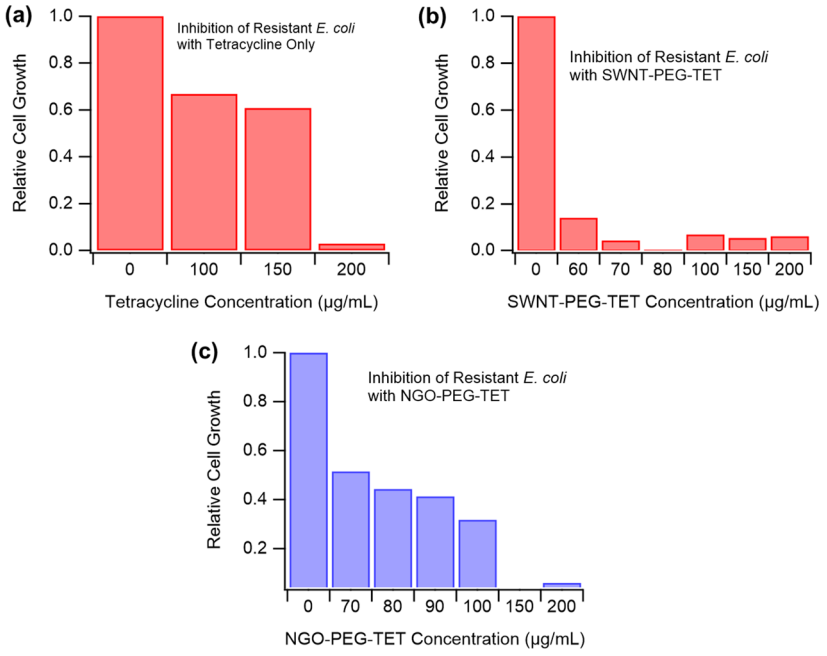

Figure 2. (a) Cell growth relative to no TET, showing inhibition of DH5α-pBR322 with tetracycline only. The MIC is 200 μg/mL. Inhibition of DH5α-pBR322 with SWNT−PEG−TET. The MIC is 70 μg/mL SWNT−PEG−TET, which corresponds to 38 μg/mL TET. (c) Inhibition of DH5α-pBR322 with NGO−PEG−TET. The MIC is 150 μg/mL NGO−PEG−TET, which corresponds to 75 μg/mL TET.

https://dx.doi.org/10.1021/acsanm.0c00677
ACS Appl. Nano Mater. XXXX, XXX, XXX−XXX

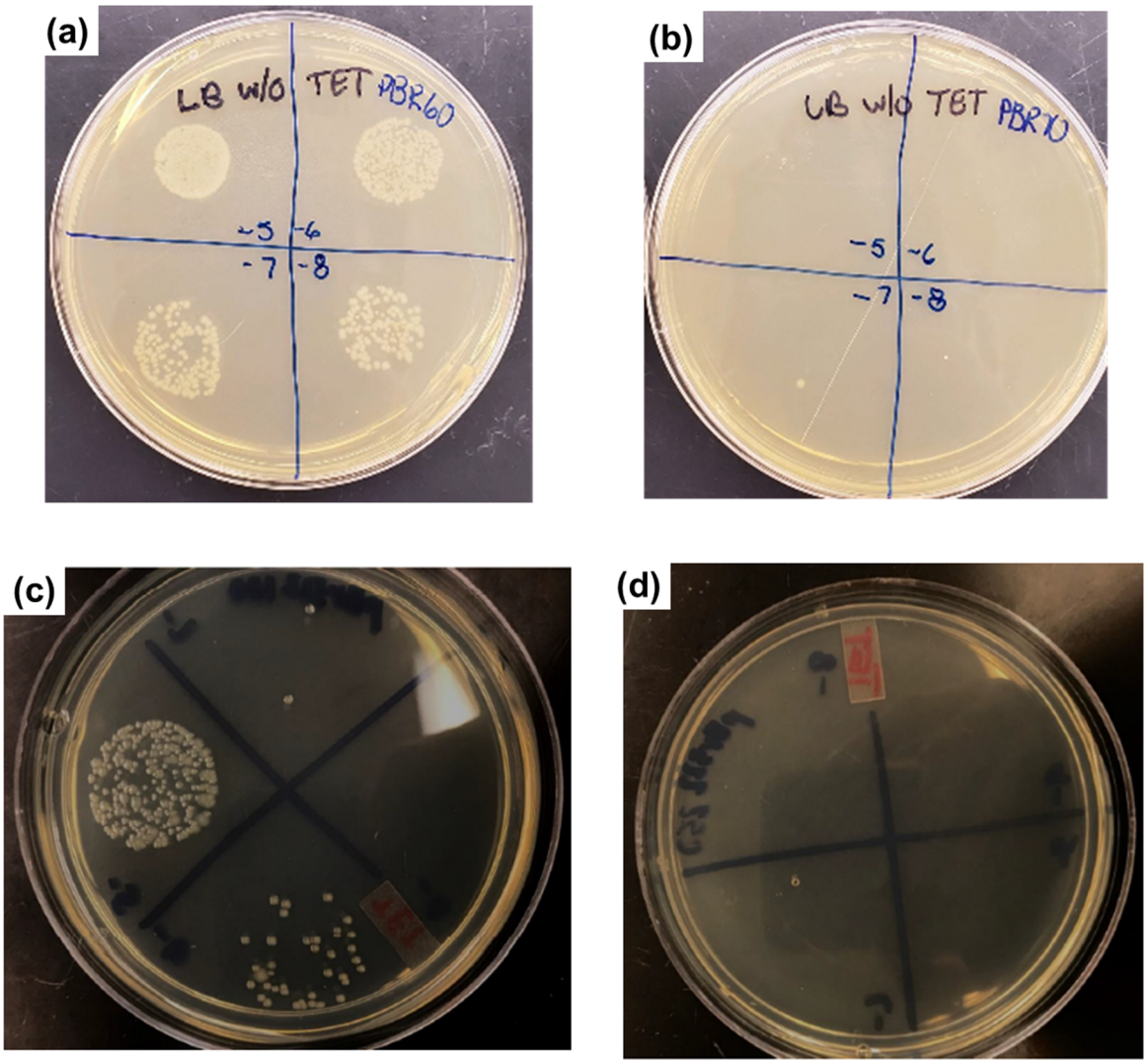

Figure 3. DH5α-pBR322 *E. coli* growth after incubation with (a) SWNT−PEG−TET at a concentration of 60 μg/mL. The dilutions plated were 10^{-5} (top left), 10^{-6} (top right), 10^{-7} (bottom left), and 10^{-8} (bottom right); (b) SWNT−PEG−TET at a concentration of 70 μg/mL. The dilutions plated were 10^{-5} (top left), 10^{-6} (top right), 10^{-7} (bottom left), and 10^{-8} (bottom right); (c) NGO−PEG−TET at a concentration of 100 μg/mL. The dilutions plated were 10^{-5} (left), 10^{-6} (bottom), 10^{-7} (top), and 10^{-8} (right); (d) NGO−PEG−TET at a concentration of 150 μg/mL. The dilutions plated were 10^{-5} (top right), 10^{-6} (bottom right), 10^{-7} (bottom left), and 10^{-8} (top left).

Table 3. Viable Counts after 24-h Incubation of DH5α-pBR322 with SWNTs−PEG−TET of Various Concentrations[a]

SWNT−PEG−TET concn (μg/mL)	dilution factor				
	1	10^{-5}	10^{-6}	10^{-7}	10^{-8}
0	TNTC	TNTC	TNTC	TNTC	TNTC
60	TNTC	TNTC	TNTC	TNTC	TNTC
70	40	1	1	1	0
80	0	0	0	0	0
100	0	0	0	0	0

[a]TNTC = too numerous to count.

Table 4. Viable Counts after 24-h Incubation of DH5α-pBR322 with NGO−PEG−TET of Various Concentrations[a]

NGO−PEG−TET concn (μg/mL)	dilution factor				
	1	10^{-5}	10^{-6}	10^{-7}	10^{-8}
0	TNTC	TNTC	TNTC	11	2
70	TNTC	TNTC	62	6	0
80	TNTC	TNTC	43	7	3
90	TNTC	TNTC	55	7	0
100	TNTC	TNTC	43	2	0
150	0	0	0	0	0
250	0	0	0	0	0

[a]TNTC = too numerous to count.

100 μg/mL but are completely inhibited at 150 μg/mL (effective TET concentration of 75 μg/mL). At these concentrations, no bacterial colonies were visible on the plates, indicating that no living bacteria were present. It is noteworthy that for both nanomaterials, the nanomaterial−TET concentration needed to inhibit the growth of the resistant strain was definitely less than the pure TET concentration of 200 μg/mL necessary to inhibit the same strain. These results illustrate that the nanomaterial plays a very important role in supporting the ability of TET to impede bacterial growth.

https://dx.doi.org/10.1021/acsanm.0c00677
ACS Appl. Nano Mater. XXXX, XXX, XXX−XXX

These results are in very good agreement with those of Khazi-Syed et al., who found that SWNTs could deliver methicillin and doxycycline to methicillin-resistant *S. epidermidis*.[39] They found that their SWNT/methicillin complex was 40 times more effective than methicillin alone. The work of Khazi-Syed et al. was published while the present work was under peer review, so it seems that their group and our group independently conceived of and tested the noncovalent attachment of antibiotics to SWNTs for use against antibiotic-resistant bacteria. The success of this approach in both studies indicates its strong potential as a means to combat antibiotic resistance. However, it is worth noting several important/key differences between the studies. First, Khazi-Syed et al. used Gram-positive *S. epidermidis*, whereas we used Gram-negative *E. coli*. Gram-negative bacteria have a significantly different cell envelope that presents a challenging barrier to antibiotic delivery. Second, they used raw, unfunctionalized HiPCO SWNTs, whereas we used acid-cut, PEG-functionalized SWNTs as well as PEG-functionalized NGO. Third, their strain of *S. epidermidis* is resistant at antibiotic concentrations of <10 μg/mL, whereas our strain is resistant at concentrations greater than 100 μg/mL. Finally, Khazi-Syed et al. used the water-soluble (hydrochloride) forms of the antibiotics, whereas we used the slightly soluble (nonhydrochloride) form of TET. The fact that major experimental differences still yield effective antibiotic-delivery nanomaterials suggests that a broad range of nanocomposite synthesis parameters could be utilized. It is particularly noteworthy that the approach has been shown to be effective for both Gram-negative and Gram-positive bacteria. Nevertheless, the importance of these differences should be further studied to improve our understanding of carbon nanomaterials as antibiotic-delivery systems.

For the system studied here, several possible mechanisms of nanomaterial action are possible. Because SWNTs[81] and graphene[82] are known to enter many cell types, one possibility is that the nanomaterials enter the cells and directly deliver the TET to the bacteria. In this way, the SWNTs or NGO could bypass and/or overwhelm the efflux pumps. Another possibility is that some TET detaches from the SWNTs in solution, and the SWNTs enter the cells, creating holes in the membrane through which the TET could then enter.

This second hypothesis was tested by adding SWNT−PEG or NGO−PEG in concentrations ranging from 0 to 100 μg/mL to cell media. After 1 h, TET was added to make a solution concentration of 100 μg/mL. (This concentration is below the MIC of TET alone but in the range where inhibition was observed for the nanomaterial−TET composites.) Growth of bacteria was assessed after 24 h. As shown in Figure S9, unattached TET in the presence of the nanomaterial did not inhibit the resistant strain of *E. coli* to any greater extent than free TET. These results demonstrate the high importance of having the antibiotic attached to the nanomaterial for delivery into the cells. These results differ from those of Gao et al., who found that their graphene oxide damaged the bacteria and made them more susceptible to the antibiotics they tested. Again, the important difference appears to be that our NGO and SWNTs are PEGylated, which appears to minimize harm to the bacteria in our studies.

Guo et al. found that unfunctionalized NGO was somewhat toxic to *E. coli* at concentrations of 80−100 μg/mL.[83] They also found that NGO significantly reduced the level of resistance-conferring genes, including the *tetA* gene that was used in the present research. However, our live/dead cell assays, the separate addition of NGO−PEG and TET results, and the LDH assay results all suggest that our NGO−PEG is no more toxic to *E. coli* than to the control. Again, an important dissimilarity between our nanomaterial and that of Guo et al. is the attachment of PEG to our NGO. This difference strongly suggests that unfunctionalized NGO might have stronger antimicrobial properties than NGO−PEG.

Our results, then, suggest that large nanomaterials such as SWNT−PEG and NGO−PEG can be used to deliver antibiotics and circumvent the efflux pump mechanism of resistance. On the basis of the research noted above, it seems likely that the SWNT−PEG and NGO−PEG enter the bacteria. The nanomaterials used are much larger than the efflux pump membrane proteins, which suggests that the nanomaterials are unable to be removed from the cell by this mechanism. If the nanomaterials can enter the cells with the TET attached, some of the TET may enter the cytoplasm and interact with the ribosomes before it can be removed by the efflux pump. Because this process depends on the size of the nanomaterial, it is expected to be broadly effective against efflux pumps in other bacterial species. On the other hand, this method is not expected to be effective against other mechanisms of antibiotic resistance, such as target modification or enzyme degradation of the antibiotic. We are currently studying organisms with these resistance mechanisms to test this hypothesis.

An interesting question is whether the SWNT−PEG−TET and/or the NGO−PEG−TET could disrupt antibiotic-resistant *E. coli* biofilms. Rodrigues and Elimelech found that unfunctionalized SWNTs at concentrations of 200−500 μg/mL disrupted nonresistant *E. coli* biofilms.[48] It is important to note that the SWNTs used in that study were significantly longer (20−50 μm) than the ones in this study. They were also used at higher concentrations and were not PEGylated. While it is plausible that SWNT−PEG−TET and/or NGO−PEG−TET could inhibit biofilms, these differences make direct comparison between studies impossible. However, because biofilm formation is an important aspect of bacteria growth, future research in our group will study the effects of SWNT−PEG−TET and NGO−PEG−TET on biofilms of resistant *E. coli*.

We note that the SWNT−PEG−TET had a much lower MIC than did the NGO−PEG−TET. Because the two materials have similar mass percentages of TET, the difference is not caused by the SWNT−PEG−TET delivering more TET to the bacteria. Rather, the important difference between the SWNT−PEG and the NGO−PEG is their shape. The SWNTs are more needle-like, and it has been shown that the narrower the needle, the more likely it is to penetrate a bacterial cell.[84] Our results, therefore, are important for the future design of nanomaterials to deliver antibiotics: cylinder-like nanomaterials are likely to be more effective than wider, flatter materials. Therefore, nanorods of any material are more likely to be effective for this task than nanosheets. This information can be of great use in the design of nanomaterials to deliver antibiotics.

CONCLUSIONS

We have demonstrated the ability of biocompatible SWNT−PEG and NGO−PEG to deliver antibiotics to Gram-negative bacteria and circumvent the efflux pump method of antibiotic resistance. SWNT−PEG and NGO−PEG are biocompatible

https://dx.doi.org/10.1021/acsanm.0c00677
ACS Appl. Nano Mater. XXXX, XXX, XXX−XXX

and do little harm to the bacteria themselves. We conclude that the nanomaterials transport the TET into the bacteria where it can bind to the ribosome before being pumped out. The SWNT−PEG material showed a greater efficacy in inhibiting the resistant bacteria than the NGO−PEG, which is likely due to the cylindrical shape of the nanotubes. These results demonstrate that nanomaterials can be used to deliver antibiotics and circumvent the efflux pump resistance mechanism. Biocompatible carbon nanomaterial delivery mechanisms can extend the life of current antibiotics and provide a useful tool in the fight against antimicrobial resistance.

■ ASSOCIATED CONTENT

Supporting Information

The Supporting Information is available free of charge at https://pubs.acs.org/doi/10.1021/acsanm.0c00677.

TEM images of SWNTs and NGO, analysis of nanomaterial size, results of control experiments of exposure of bacteria to nanomaterials, results of LDH assay experiments, NMR and FTIR spectra of nanomaterials, analysis of amount of TET attached to nanomaterials, and results of exposure of bacteria to nanomaterials followed by TET (PDF)

■ AUTHOR INFORMATION

Corresponding Author

Mark D. Ellison − *Department of Chemistry, Ursinus College, Collegeville, Pennsylvania 19426, United States;* orcid.org/0000-0003-3201-8478; Email: mellison@ursinus.edu

Authors

Jordan A. Carver − *Department of Chemistry, Ursinus College, Collegeville, Pennsylvania 19426, United States*

Audrey L. Simpson − *Department of Chemistry, Ursinus College, Collegeville, Pennsylvania 19426, United States*

Ria P. Rathi − *Department of Chemistry, Ursinus College, Collegeville, Pennsylvania 19426, United States*

Nerica Normil − *Department of Chemistry, Ursinus College, Collegeville, Pennsylvania 19426, United States*

Amy G. Lee − *Department of Chemistry, Ursinus College, Collegeville, Pennsylvania 19426, United States*

Madison D. Force − *Department of Chemistry, Ursinus College, Collegeville, Pennsylvania 19426, United States*

Katherine A. Fiocca − *Department of Chemistry, Ursinus College, Collegeville, Pennsylvania 19426, United States*

Christopher E. Maley − *Department of Chemistry, Ursinus College, Collegeville, Pennsylvania 19426, United States*

Kara M. DiJoseph − *Department of Chemistry, Ursinus College, Collegeville, Pennsylvania 19426, United States*

Abigail L. Goldstein − *Department of Biology and Department of Chemistry, Ursinus College, Collegeville, Pennsylvania 19426, United StatesDepartment of Chemistry and Department of Biology, Ursinus College, Collegeville, Pennsylvania 19426, United States*

Amin A. Attari − *Department of Chemistry, Ursinus College, Collegeville, Pennsylvania 19426, United States*

Haley L. O'Malley − *Department of Chemistry, Ursinus College, Collegeville, Pennsylvania 19426, United States*

Jaclyn G. Zaccaro − *Department of Chemistry, Ursinus College, Collegeville, Pennsylvania 19426, United States*

Noël M. McCampbell − *Department of Chemistry, Ursinus College, Collegeville, Pennsylvania 19426, United States*

Christina A. Wentz − *Department of Chemistry, Ursinus College, Collegeville, Pennsylvania 19426, United States*

Jessica E. Long − *Department of Chemistry, Ursinus College, Collegeville, Pennsylvania 19426, United States*

Lilly M. McQueen − *Department of Chemistry, Ursinus College, Collegeville, Pennsylvania 19426, United States*

Francis J. Sirch − *Department of Chemistry, Ursinus College, Collegeville, Pennsylvania 19426, United States*

Broderick K. Johnson − *Department of Chemistry, Ursinus College, Collegeville, Pennsylvania 19426, United States*

Molly E. Divis − *Department of Chemistry, Ursinus College, Collegeville, Pennsylvania 19426, United States*

Matthew L. Chorney − *Department of Chemistry, Ursinus College, Collegeville, Pennsylvania 19426, United States*

Steven L. DiStefano − *Department of Chemistry, Ursinus College, Collegeville, Pennsylvania 19426, United States*

Holly M. Yost − *Department of Chemistry, Ursinus College, Collegeville, Pennsylvania 19426, United States*

Brandon L. Greyson − *Department of Chemistry, Ursinus College, Collegeville, Pennsylvania 19426, United States*

Emily A. Cid − *Department of Chemistry, Ursinus College, Collegeville, Pennsylvania 19426, United States*

Kyumin Lee − *Department of Chemistry, Ursinus College, Collegeville, Pennsylvania 19426, United States*

Codi J. Yhap − *Department of Chemistry, Ursinus College, Collegeville, Pennsylvania 19426, United States*

Michelle Dong − *Department of Chemistry, Ursinus College, Collegeville, Pennsylvania 19426, United States*

Dayna L. Thomas − *Department of Chemistry, Ursinus College, Collegeville, Pennsylvania 19426, United States*

Brittany E. Banks − *Department of Chemistry, Ursinus College, Collegeville, Pennsylvania 19426, United States*

Regan B. Newman − *Department of Chemistry, Ursinus College, Collegeville, Pennsylvania 19426, United States*

Jailene Rodriguez − *Department of Chemistry, Ursinus College, Collegeville, Pennsylvania 19426, United States*

Alix T. Segil − *Department of Chemistry, Ursinus College, Collegeville, Pennsylvania 19426, United States*

Justin A. Siberski − *Department of Chemistry, Ursinus College, Collegeville, Pennsylvania 19426, United States*

Anthony L. Lobo − *Department of Biology, Ursinus College, Collegeville, Pennsylvania 19426, United States*

Complete contact information is available at: https://pubs.acs.org/10.1021/acsanm.0c00677

Author Contributions

#These authors contributed equally.

Notes

The authors declare no competing financial interest.

■ ACKNOWLEDGMENTS

The authors acknowledge Ursinus College and the Ursinus College Summer Fellows Program for financial support and Ann Breen and Matt Zrada for assistance. M.D.E. acknowledges Dr. Kate Plass of Franklin and Marshall College for assistance in collecting the TEM images. The TEM images were collected on an instrument purchased through NSF MRI Award CHE-1724948. The NMR spectra were collected on an instrument purchased through NSF MRI Award CHE-

https://dx.doi.org/10.1021/acsanm.0c00677
ACS Appl. Nano Mater. XXXX, XXX, XXX−XXX

1726836. We acknowledge Erica Ellison for a critical proofreading of the manuscript.

REFERENCES

(1) About Antimicrobial Resistance. https://www.cdc.gov/drugresistance/about.html (accessed 2020/03/26).

(2) *No Time to Wait: Securing the Future from Drug-Resistant Infections*; World Health Organization: New York, 2019.

(3) Jonas, O. B.; Irwin, A.; Berthe, F. C. J.; Le Gall, F. G.; Marquez, P. V. *Drug-Resistant Infections: A Threat to Our Economic Future*, Final Report (English); World Bank Group: Washington, DC, 2017; Vol. 2

(4) Perros, M. A Sustainable Model for Antibiotics. *Science* **2015**, *347*, 1062−1064.

(5) Walsh, C.; Wencewicz, T. *Antibiotics: Challenges, Mechanisms, Opportunities*; American Society for Microbiology: Washington, DC, 2016; p 477.

(6) *Global Antimicrobial Resistance Surveillance System (Glass) Report: Early Implementation 2016−17*; World Health Organization: Geneva, 2017; pp Licence: CC BY-NC-SA 3.0 IGO.

(7) Sutcliffe, J. G. Complete Nucleotide Sequence of the Escherichia Coli Plasmid Pbr322. *Cold Spring Harbor Symp. Quant. Biol.* **1979**, *43*, 77−90.

(8) Sun, J.; Deng, Z.; Yan, A. Bacterial Multidrug Efflux Pumps: Mechanisms, Physiology and Pharmacological Exploitations. *Biochem. Biophys. Res. Commun.* **2014**, *453*, 254−267.

(9) Stavropoulos, T. A.; Strathdee, C. A. Expression of the *Teta*(C) Tetracycline Efflux Pump in *Escherichia Coli* Confers Osmotic Sensitivity. *FEMS Microbiol. Lett.* **2000**, *190*, 147−150.

(10) Baptista, P. V.; McCusker, M. P.; Carvalho, A.; Ferreira, D. A.; Mohan, N. M.; Martins, M.; Fernandes, A. R. Nano-Strategies to Fight Multidrug Resistant Bacteria-″a Battle of the Titans″. *Front. Microbiol.* **2018**, *9*, 1441.

(11) Hemeg, H. A. Nanomaterials for Alternative Antibacterial Therapy. *Int. J. Nanomed.* **2017**, *12*, 8211−8225.

(12) Huh, A. J.; Kwon, Y. J. ″Nanoantibiotics″: A New Paradigm for Treating Infectious Diseases Using Nanomaterials in the Antibiotics Resistant Era. *J. Controlled Release* **2011**, *156*, 128−145.

(13) Bhirde, A. A.; Patel, V.; Gavard, J.; Zhang, G.; Sousa, Đ. A. A.; Masedunskas, A.; Leapman, R. D.; Weigert, Đ. R.; Gutkind, J. S.; Rusling, J. F. Targeted Killing of Cancer Cells in Vivo Nanotube-Based Drug Delivery. *ACS Nano* **2009**, *3*, 307−316.

(14) Feazell, R. P.; Nakayama-Ratchford, N.; Dai, H.; Lippard, S. J. Soluble Single-Walled Carbon Nanotubes as Longboat Delivery Systems for Platinum(IV) Anticancer Drug Design. *J. Am. Chem. Soc.* **2007**, *129*, 8438−8439.

(15) Kam, N. W. S.; O'Connell, M.; Wisdom, J. A.; Dai, H. Carbon Nanotubes as Multifunctional Biological Transporters and near-Infrared Agents for Selective Cancer Cell Destruction. *Proc. Natl. Acad. Sci. U. S. A.* **2005**, *102*, 11600−11605.

(16) Lee, P. C.; Chiou, Y. C.; Wong, J. M.; Peng, C. L.; Shieh, M. J. Targeting Colorectal Cancer Cells with Single-Walled Carbon Nanotubes Conjugated to Anticancer Agent Sn-38 and Egfr Antibody. *Biomaterials* **2013**, *34*, 8756−8765.

(17) Liu, Z.; Chen, K.; Davis, C.; Sherlock, S.; Cao, Q.; Chen, X.; Dai, H. Drug Delivery with Carbon Nanotubes for *in Vivo* Cancer Treatment. *Cancer Res.* **2008**, *68*, 6652−6660.

(18) Liu, Z.; Robinson, J. T.; Sun, X.; Dai, H. Pegylated Nanographene Oxide for Delivery of Water-Insoluble Cancer Drugs. *J. Am. Chem. Soc.* **2008**, *130*, 10876−10877.

(19) Bianco, A.; Kostarelos, K.; Prato, M. Applications of Carbon Nanotubes in Drug Delivery. *Curr. Opin. Chem. Biol.* **2005**, *9*, 674−679.

(20) Bianco, A.; Prato, M. Can Carbon Nanotubes Be Considered Useful Tools for Biological Applications? *Adv. Mater.* **2003**, *15*, 1765−1768.

(21) Pantarotto, D.; Briand, J.-P.; Prato, M.; Bianco, A. Translocation of Bioactive Peptides across Cell Membranes by Carbon Nanotubes. *Chem. Commun.* **2004**, 16−17.

(22) Pantarotto, D.; Singh, R.; McCarthy, D.; Erhardt, M.; Briand, J.-P.; Prato, M.; Kostarelos, K.; Bianco, A. Functionalized Carbon Nanotubes for Plasmid DNA Gene Delivery. *Angew. Chem., Int. Ed.* **2004**, *43*, 5242−5246.

(23) Prato, M.; Kostarelos, K.; Bianco, A. Functionalized Carbon Nanotubes in Drug Design and Discovery. *Acc. Chem. Res.* **2008**, *41*, 60−68.

(24) Dhar, S.; Liu, Z.; Thomale, J.; Dai, H.; Lippard, S. J. Targeted Single-Wall Carbon Nanotube-Mediated Pt(Iv) Prodrug Delivery Using Folate as a Homing Device. *J. Am. Chem. Soc.* **2008**, *130*, 11467−11476.

(25) Liu, Z.; Cai, W.; He, L.; Nozomi, N.; Chen, K.; Sun, X.; Chen, X.; Dai, H. *In Vivo* Biodistribution and Highly Efficient Tumour Targeting of Carbon Nanotubes in Mice. *Nat. Nanotechnol.* **2007**, *2*, 47−52.

(26) Liu, Z.; Sun, X.; Nakayama-Ratchford, N.; Dai, H. Supramolecular Chemistry on Water-Soluble Carbon Nanotubes for Drug Loading and Delivery. *ACS Nano* **2007**, *1*, 50−56.

(27) Liu, Z.; Tabakman, S.; Welsher, K.; Dai, H. Carbon Nanotubes in Biology and Medicine: *In Vitro* and *in Vivo* Detection, Imaging, and Drug Delivery. *Nano Res.* **2009**, *2*, 85−120.

(28) Cheng, Y.; Samia, A. C.; Meyers, J. D.; Panagopoulos, I.; Fei, B.; Burda, C. Highly Efficient Drug Delivery with Gold Nanoparticle Vectors for in Vivo Photodynamic Therapy of Cancer. *J. Am. Chem. Soc.* **2008**, *130*, 10643−10647.

(29) De Jong, W. H.; Borm, P. J. A. Drug Delivery and Nanoparticles: Applications and Hazards. *Int. J. Nanomed.* **2008**, *3*, 133−149.

(30) Sahoo, S. K.; Labhasetwar, V. Nanotech Approaches to Drug Delivery and Imaging. *Drug Discovery Today* **2003**, *8*, 1112−1120.

(31) Benincasa, M.; Pacor, S.; Wu, W.; Prato, M.; Bianco, A.; Gennaro, R. Antifungal Activity of Amphotericin B Conjugated to Carbon Nanotubes. *ACS Nano* **2011**, *5*, 199−208.

(32) Wu, W.; Wieckowski, S.; Pastorin, G.; Benincasa, M.; Klumpp, C.; Briand, J.-P.; Gennaro, R.; Prato, M.; Bianco, A. Targeted Delivery of Amphotericin B to Cells by Using Functionalized Carbon Nanotubes. *Angew. Chem., Int. Ed.* **2005**, *44*, 6358−6362.

(33) Assali, M.; Zaid, A. N.; Abdallah, F.; Almasri, M.; Khayyat, R. Single-Walled Carbon Nanotubes-Ciprofloxacin Nanoantibiotic: Strategy to Improve Ciprofloxacin Antibacterial Activity. *Int. J. Nanomed.* **2017**, *12*, 6647−6659.

(34) Thakur, M.; Pandey, S.; Mewada, A.; Patil, V.; Khade, M.; Goshi, E.; Sharon, M. Antibiotic Conjugated Fluorescent Carbon Dots as a Theranostic Agent for Controlled Drug Release, Bioimaging, and Enhanced Antimicrobial Activity. *J. Drug Delivery* **2014**, *2014*, 9.

(35) Ghosh, D.; Chandra, S.; Chakraborty, A.; Ghosh, S. K.; Pramanik, P. A Novel Graphene Oxide-Para Amino Benzoic Acid Nanosheet as Effective Drug Delivery System to Treat Drug Resistant Bacteria. *Int. J. Pharm. Sci. Drug Res.* **2010**, *2*, 127−133.

(36) Gao, Y.; Wu, J.; Ren, X.; Tan, X.; Hayat, T.; Alsaedi, A.; Cheng, C.; Chen, C. Impact of Graphene Oxide on the Antibacterial Activity of Antibiotics against Bacteria. *Environ. Sci.: Nano* **2017**, *4*, 1016−1024.

(37) Yousefi, M.; Dadashpour, M.; Hejazi, M.; Hasanzadeh, M.; Behnam, B.; de la Guardia, M.; Shadjou, N.; Mokhtarzadeh, A. Anti-Bacterial Activity of Graphene Oxide as a New Weapon Nanomaterial to Combat Multidrug-Resistance Bacteria. *Mater. Sci. Eng., C* **2017**, *74*, 568−581.

(38) Guo, M.-T.; Zhang, G.-S. Graphene Oxide in the Water Environment Could Affect Tetracycline-Antibiotic Resistance. *Chemosphere* **2017**, *183*, 197−203.

(39) Khazi-Syed, A.; Hasan, M. T.; Campbell, E.; Gonzalez-Rodriguez, R.; Naumov, A. V. Single-Walled Carbon Nanotube-Assisted Antibiotic Delivery and Imaging in S. Epidermidis Strains Addressing Antibiotic Resistance. *Nanomaterials* **2019**, *9*, 1685.

(40) Liu, Y.; Zhao, Y.; Sun, B.; Chen, C. Understanding the Toxicity of Carbon Nanotubes. *Acc. Chem. Res.* **2013**, *46*, 702−713.

https://dx.doi.org/10.1021/acsanm.0c00677
ACS Appl. Nano Mater. XXXX, XXX, XXX−XXX

(41) Sayes, C. M.; Liang, F.; Hudson, J. L.; Mendez, J.; Guo, W.; Beach, J. M.; Moore, V. C.; Doyle, C. D.; West, J. L.; Billups, W. E.; Ausman, K. D.; Colvin, V. L. Functionalization Density Dependence of Single-Walled Carbon Nanotubes Cytotoxicity in Vitro. *Toxicol. Lett.* **2006**, *161*, 135−142.
(42) Donaldson, K.; Poland, C. A. Nanotoxicology: New Insights into Nanotubes. *Nat. Nanotechnol.* **2009**, *4*, 708−710.
(43) Kostarelos, K. The Long and Short of Carbon Nanotube Toxicity. *Nat. Biotechnol.* **2008**, *26*, 774−776.
(44) Lam, C.-W.; James, J. T.; McCluskey, R.; Hunter, R. L. Pulmonary Toxicity of Single-Wall Carbon Nanotubes in Mice 7 and 90 Days after Intratracheal Instillation. *Toxicol. Sci.* **2003**, *77*, 126−134.
(45) Lindberg, H. K.; Falck, G. C.-M.; Suhonen, S.; Vippola, M.; Vanhala, E.; Catalan, J.; Savolainan, K.; Norppa, H. Genotoxicity of Nanomaterials: DNA Damage and Micronuclei Induced by Carbon Nanotubes and Graphite Nanofibres in Human Bronchial Epithelial Cells in Vitro. *Toxicol. Lett.* **2009**, *186*, 166−173.
(46) Kang, B.; Yu, D.-c.; Chang, S.-q.; Chen, D.; Dai, Y.-d.; Ding, Y. Intracellular Uptake, Trafficking and Subcellular Distribution of Folate-Conjugated Single-Walled Carbon Nanotubes within Living Cells. *Nanotechnology* **2008**, *19*, 1−8.
(47) Kang, S.; Herzberg, M.; Rodrigues, D. F.; Elimelech, M. Antibacterial Effects of Carbon Nanotubes: Size Does Matter! *Langmuir* **2008**, *24*, 6409−6413.
(48) Rodrigues, D. F.; Elimelech, M. Toxic Effects of Single-Walled Carbon Nanotubes in the Development of E. Coli Biofilm. *Environ. Sci. Technol.* **2010**, *44*, 4583−4589.
(49) Liao, C.; Li, Y.; Tjong, S. C. Graphene Nanomaterials: Synthesis, Biocompatibility, and Cytotoxicity. *Int. J. Mol. Sci.* **2018**, *19*, 3564.
(50) Liao, K. H.; Lin, Y. S.; Macosko, C. W.; Haynes, C. L. Cytotoxicity of Graphene Oxide and Graphene in Human Erythrocytes and Skin Fibroblasts. *ACS Appl. Mater. Interfaces* **2011**, *3*, 2607−2615.
(51) Pelin, M.; Fusco, L.; Leon, V.; Martin, C.; Criado, A.; Sosa, S.; Vazquez, E.; Tubaro, A.; Prato, M. Differential Cytotoxic Effects of Graphene and Graphene Oxide on Skin Keratinocytes. *Sci. Rep.* **2017**, *7*, 40572.
(52) Bussy, C.; Ali-Boucetta, H.; Kostarelos, K. Safety Considerations for Graphene: Lessons Learnt from Carbon Nanotubes. *Acc. Chem. Res.* **2013**, *46*, 692−701.
(53) Akhavan, O.; Ghaderi, E. Toxicity of Graphene and Graphene Oxide Nanowalls against Bacteria. *ACS Nano* **2010**, *4*, 5731−5736.
(54) Dumortier, H.; Lacotte, S.; Pastorin, G.; Marega, R.; Wu, W.; Bonifazi, D.; Briand, J.-P.; Prato, M.; Muller, S.; Bianco, A. Functionalized Carbon Nanotubes Are Non-Cytotoxic and Preserve the Functionality of Primary Immune Cells. *Nano Lett.* **2006**, *6*, 1522−1528.
(55) Goodwin, C. M.; Lewis, G. G.; Fiorella, A.; Ellison, M. D.; Kohn, R. Synthesis and Toxicity Testing of Cysteine-Functionalized Single-Walled Carbon Nanotubes with *Caenorhabditis Elegans*. *RSC Adv.* **2014**, *4*, 5893−5900.
(56) Seabra, A. B.; Paula, A. J.; de Lima, R.; Alves, O. L.; Duran, N. Nanotoxicity of Graphene and Graphene Oxide. *Chem. Res. Toxicol.* **2014**, *27*, 159−168.
(57) Brodersen, D. E.; Clemons, W. M.; Carter, A. P.; Morgan-Warren, R. J.; Wimberly, B. T.; Ramakrishnan, V. The Structural Basis for the Action of the Antibiotics Tetracycline, Pactamycin, and Hygromycin B on the 30s Ribosomal Subunit. *Cell* **2000**, *103*, 1143−1154.
(58) Maxwell, I. H. Partial Removal of Bound Transfer Rna from Polysomes Engaged in Protein Synthesis *in Vitro* after Addition of Tetracycline. *Biochim. Biophys. Acta, Nucleic Acids Protein Synth.* **1967**, *138*, 337−346.
(59) Bergmann, C. P.; Machado, F. M. *Carbon Nanomaterials as Adsorbents for Environmental and Biological Applications*; Springer: New York, 2015.
(60) Ghadim, E. E.; Manouchehri, F.; Soleimani, G.; Hosseini, H.; Kimiagar, S.; Nafisi, S. Adsorption Properties of Tetracycline onto Graphene Oxide: Equilibrium, Kinetic and Thermodynamic Studies. *PLoS One* **2013**, *8*, e79254.
(61) Kolosnjaj-Tabi, J.; Hartman, K. B.; Boudjemaa, S.; Ananta, J. S.; Morgant, G.; Szwarc, H.; Wilson, L. J.; Moussa, F. *In Vivo* Behavior of Large Doses of Ultrashort and Full-Length Single-Walled Carbon Nanotubes after Oral and Intraperitoneal Administration to Swiss Mice. *ACS Nano* **2010**, *4*, 1481−1492.
(62) Shuba, M. V.; Paddubskaya, A. G.; Kuzhir, P. P.; Maksimenko, S. A.; Ksenevich, V. K.; Niaura, G.; Seliuta, D.; Kasalynas, I.; Valusis, G. Soft Cutting of Single-Wall Carbon Nanotubes by Low Temperature Ultrasonication in a Mixture of Sulfuric and Nitric Acids. *Nanotechnology* **2012**, *23*, 495714.
(63) Schindelin, J.; Arganda-Carreras, I.; Frise, E.; Kaynig, V.; Longair, M.; Pietzsch, T.; Preibisch, S.; Rueden, C.; Saalfeld, S.; Schmid, B.; Tinevez, J.-Y.; White, D. J.; Hartenstein, V.; Eliceiri, K.; Tomancak, P.; Cardona, A. Fiji: An Open-Source Platform for Biological-Image Analysis. *Nat. Methods* **2012**, *9*, 676.
(64) Zhang, X.; Shen, J.; Zhuo, N.; Tian, Z.; Xu, P.; Yang, Z.; Yang, W. Interactions between Antibiotics and Graphene-Based Materials in Water: A Comparative Experimental and Theoretical Investigation. *ACS Appl. Mater. Interfaces* **2016**, *8*, 24273−24280.
(65) Bauer, M. E.; Welch, R. A. Association of Rtx Toxins with Erythrocytes. *Infect. Immun.* **1996**, *64*, 4665−4672.
(66) Yamanaka, H.; Shimatani, S.; Tanaka, M.; Katsu, T.; Ono, B.-i.; Shinoda, S. Susceptibility of Erythrocytes from Several Animal Species to Vibrio Vulnificus Hemolysin. *FEMS Microbiol. Lett.* **1989**, *61*, 251−255.
(67) Dennison, S. R.; Phoenix, D. A. Susceptibility of Sheep, Human, and Pig Erythrocytes to Haemolysis by the Antimicrobial Peptide Modelin 5. *Eur. Biophys. J.* **2014**, *43*, 423−432.
(68) He, J.; Luo, X.; Jin, D.; Wang, Y.; Zhang, T. Identification, Recombinant Expression, and Characterization of Lgh2, a Novel Antimicrobial Peptide of Lactobacillus Casei Hz1. *Molecules* **2018**, *23*, 2246.
(69) Hisano, M.; Ashida, A.; Nakano, E.; Suehiro, M.; Yoshida, Y.; Matsumoto, M.; Miyata, T.; Fujimura, Y.; Hattori, M. Autoimmune-Type Atypical Hemolytic Uremic Syndrome Treated with Eculizumab as First-Line Therapy. *Pediatrics International* **2015**, *57*, 313−317.
(70) Yoshida, Y.; Miyata, T.; Matsumoto, M.; Shirotani-Ikejima, H.; Uchida, Y.; Ohyama, Y.; Kokubo, T.; Fujimura, Y. A Novel Quantitative Hemolytic Assay Coupled with Restriction Fragment Length Polymorphisms Analysis Enabled Early Diagnosis of Atypical Hemolytic Uremic Syndrome and Identified Unique Predisposing Mutations in Japan. *PLoS One* **2015**, *10*, e0124655.
(71) Osorio e Castro, V. R.; Ashwood, E. R.; Wood, S. G.; Vernon, L. P. Hemolysis of Erythrocytes and Fluorescence Polarization Changes Elicited by Peptide Toxins, Aliphatic Alcohols, Related Glycols and Benzylidene Derivatives. *Biochim. Biophys. Acta, Biomembr.* **1990**, *1029*, 252−258.
(72) Salvioli, G.; Gaetti, E.; Panini, R.; Lugli, R.; Pradelli, J. M. Different Resistance of Mammalian Red Blood Cells to Hemolysis by Bile Salts. *Lipids* **1993**, *28*, 999−1003.
(73) Cho, S. H.; Hong, J. H.; Noh, Y. W.; Lee, E.; Lee, C. S.; Lim, Y. T. Raspberry-Like Poly(Γ-Glutamic Acid) Hydrogel Particles for Ph-Dependent Cell Membrane Passage and Controlled Cytosolic Delivery of Antitumor Drugs. *Int. J. Nanomed.* **2016**, *11*, 5621−5632.
(74) Canapè, C.; Foillard, S.; Bonafè, R.; Maiocchi, A.; Doris, E. Comparative Assessment of the in Vitro Toxicity of Some Functionalized Carbon Nanotubes and Fullerenes. *RSC Adv.* **2015**, *5*, 68446−68453.
(75) Sasidharan, A.; Panchakarla, L. S.; Sadanandan, A. R.; Ashokan, A.; Chandran, P.; Girish, C. M.; Menon, D.; Nair, S. V.; Rao, C. N.; Koyakutty, M. Hemocompatibility and Macrophage Response of Pristine and Functionalized Graphene. *Small* **2012**, *8*, 1251−1263.
(76) Amin, K.; Dannenfelser, R.-M. *In Vitro* Hemolysis: Guidance for the Pharmaceutical Scientist. *J. Pharm. Sci.* **2006**, *95*, 1173−1176.

https://dx.doi.org/10.1021/acsanm.0c00677
ACS Appl. Nano Mater. XXXX, XXX, XXX−XXX

(77) Kang, S.; Pinault, M.; Pfefferle, L. D.; Elimelech, M. Single-Walled Carbon Nanotubes Exhibit Strong Antimicrobial Activity. *Langmuir* **2007**, *23*, 8670−8673.
(78) Yang, C.; Mamouni, J.; Tang, Y.; Yang, L. Antimicrobial Activity of Single-Walled Carbon Nanotubes: Length Effect. *Langmuir* **2010**, *26*, 16013−16019.
(79) Casy, A. F.; Yasin, A. The Identification and Stereochemical Study of Tetracycline Antibiotics by ^{1}h Nuclear Magnetic Resonance Spectroscopy. *J. Pharm. Biomed. Anal.* **1983**, *1*, 281−292.
(80) Dust, J. M.; Fang, Z. H.; Harris, J. M. Proton Nmr Characterization of Poly(Ethylene Glycols) and Derivatives. *Macromolecules* **1990**, *23*, 3742−3746.
(81) Kostarelos, K.; Lacerda, L.; Pastorin, G.; Wu, W.; Wieckowski, S.; Luangsivilay, J.; Godefroy, S.; Pantarotto, D.; Briand, J.-P.; Muller, S.; Prato, M.; Bianco, A. Cellular Uptake of Functionalized Carbon Nanotubes Is Independent of Functional Group and Cell Type. *Nat. Nanotechnol.* **2007**, *2*, 108−113.
(82) Li, Y.; Yuan, H.; von dem Bussche, A.; Creighton, M.; Hurt, R. H.; Kane, A. B.; Gao, H. Graphene Microsheets Enter Cells through Spontaneous Membrane Penetration at Edge Asperities and Corner Sites. *Proc. Natl. Acad. Sci. U. S. A.* **2013**, *110*, 12295−12300.
(83) Guo, M. T.; Zhang, G. S. Graphene Oxide in the Water Environment Could Affect Tetracycline-Antibiotic Resistance. *Chemosphere* **2017**, *183*, 197−203.
(84) Liu, S.; Wei, L.; Hao, L.; Fang, N.; Chang, M. W.; Xu, R.; Yang, Y.; Chen, Y. Sharper and Faster ″Nano Darts″ Kill More Bacteria: A Study of Antibacterial Activity of Individually Dispersed Pristine Single-Walled Carbon Nanotube. *ACS Nano* **2009**, *3*, 3891−3902.

https://dx.doi.org/10.1021/acsanm.0c00677
ACS Appl. Nano Mater. XXXX, XXX, XXX−XXX